Test of the statistical model in ^{96}Mo with the $BaF_2\gamma$ calorimeter DANCE array

S. A. Sheets,[1] U. Agvaanluvsan,[2] J. A. Becker,[2] F. Bečvář,[3] T. A. Bredeweg,[4] R. C. Haight,[4] M. Jandel,[4] M. Krtička,[3] G. E. Mitchell,[1] J. M. O'Donnell,[4] W. Parker,[2] R. Reifarth,[4] R. S. Rundberg,[4] E. I. Sharapov,[5] J. L. Ullmann,[4] D. J. Vieira,[4] J. B. Wilhelmy,[4] J. M. Wouters,[4] and C. Y. Wu[2]

[1]*North Carolina State University, Raleigh, North Carolina 27695, USA and Triangle Universities Nuclear Laboratory, Durham, North Carolina 27708, USA*

[2]*Lawrence Livermore National Laboratory, L-414, 7000 East Avenue, Livermore, California 94551, USA*

[3]*Charles University in Prague, CZ-180 00 Prague 8, Czech Republic*

[4]*Los Alamos National Laboratory, Los Alamos, New Mexico 87545, USA*

[5]*Joint Institute for Nuclear Research, RU-141980 Dubna, Russia*

(Received 29 August 2008; published 3 February 2009)

The γ-ray cascades following the ^{95}Mo$(n,\gamma)^{96}$Mo reaction were studied with the γ calorimeter DANCE (Detector for Advanced Neutron Capture Experiments) consisting of 160 BaF_2 scintillation detectors at the Los Alamos Neutron Science Center. The γ-ray energy spectra for different multiplicities were measured for s- and p-wave resonances below 2 keV. The shapes of these spectra were found to be in very good agreement with simulations using the DICEBOX statistical model code. The relevant model parameters used for the level density and photon strength functions were identical with those that provided the best fit of the data from a recent measurement of the thermal ^{95}Mo$(n,\gamma)^{96}$Mo reaction with the two-step-cascade method. The reported results strongly suggest that the extreme statistical model works very well in the mass region near $A = 100$.

DOI: 10.1103/PhysRevC.79.024301 PACS number(s): 28.20.Np, 27.60.+j, 25.40.Lw, 25.40.Ny

I. INTRODUCTION

In medium- to heavy-mass nuclei detailed spectroscopic information exists only for levels at low excitation energy near the ground state. As the number of levels increases rapidly with excitation energy, the difficulties of resolving transitions populating or depopulating the levels increase; as a consequence, our ability to obtain reliable spectroscopic information decreases. Hereafter, this excitation region is referred to as a *level quasicontinuum*. It is believed that γ decay of the nucleus in the quasicontinuum is described by the extreme statistical model in terms of the nuclear density function and a set of photon strength functions (PSFs) for different multipolarities. The most direct way to examine the validity of such an approach is via the neutron capture reaction from isolated resonances. Although the extreme statistical model may be reasonable for heavy nuclei, the validity of this approach in lighter nuclei is an open question.

The present study is an attempt to address this issue in the medium-mass nuclide ^{96}Mo. The combination of the pulsed neutron beam at LANSCE (Los Alamos Neutron Science Center) and the highly segmented, highly efficient γ calorimeter DANCE (Detector for Advanced Neutron Capture Experiments) provides an ideal opportunity to study the γ-ray cascades.

Capture cross sections for the Mo isotopes are important for fuel cycle calculations and for astrophysical applications. The Mo isotopes provide an excellent test for the applicability of the statistical model because they are in the mass region where strong nonstatistical effects have been observed and interpreted within the framework of the valence-neutron model [1].

In the present paper we describe a measurement of the ^{95}Mo$(n,\gamma)^{96}$Mo reaction using the DANCE calorimeter. In a related measurement we also studied the same reaction using the two-step cascade (TSC) method following thermal neutron capture in ^{95}Mo at the Řež Institute of Nuclear Physics [2].

These two techniques are in several respects complementary. The γ-calorimetric measurements can be performed at many *isolated* resonances of known spin and parity, while the initial state in the TSC method, based on the use of thermal neutrons, often has a contribution from several resonances. By definition the TSC method studies only multiplicity two γ cascades, whereas the DANCE detector provides information on many multiplicities. The BaF_2 detectors, forming the DANCE calorimeter, provide limited γ-ray energy resolution, but the TSC measurement uses germanium detectors with excellent resolution. The TSC measurement may thus provide information on the two-step γ decay to many levels with different spins and parities. The γ-calorimetric measurements yield information on all multiple-step cascades terminating at the ground state. The combination of measurements with these two systems should provide a detailed test of the applicability of the extreme statistical model in this mass region.

Another motivation for the study of Mo is provided by the observation of an unusual low-energy enhancement in the PSFs in a series of medium-mass nuclei. These observations were made at the Oslo Cyclotron Laboratory and used the $(^3\mathrm{He},\alpha\gamma)$ and $(^3\mathrm{He},{}^3\mathrm{He}'\gamma)$ reactions and the sequential extraction procedure, now often called the "Oslo method," to extract the sum of PSFs as a function of γ-ray energy E_γ and the nuclear level density as a function of excitation energy E. The large enhancement for energies $1 \lesssim E_\gamma \lesssim 3$ MeV was first observed in ^{56,57}Fe [3,4], and later in a series of nuclei—^{50,51}V [5], $^{93-98}$Mo [6,7], and ^{44,45}Sc [8]. The low-energy enhancement has been called a *soft pole*.

The extra photon strength reported in Refs. [3–8] has been observed for all 12 nuclei with $A < 100$ studied so far from the ^{3}He-induced γ emission. It should also be noted that no

low-energy enhancement in the PSFs has been observed in nuclei with masses greater than $A = 100$.

Recently, Guttormsen and co-workers [9] have performed a reanalysis of the ^{96}Mo data and obtained a reduced low-energy enhancement. Therefore in the present paper we compare our experimental results only with their latest version of the photon strength function.

In this paper we address the general issue of the applicability of the extreme statistical model in this mass region. In an earlier report [10] the spins and parities of isolated resonances in ^{96}Mo were determined. In the present analysis we examine the cascade γ decay following neutron capture at well-isolated strong resonances of known spin and parity. We compare the cascade data with model simulations performed using the DICEBOX algorithm described in Sec. III. In addition to the multiplicity two data used for spectroscopic purposes in Ref. [10], we also considered higher multiplicity spectra. We focus on comparison of model simulations with the cascade data. In Sec. II the experimental technique to measure the γ spectra is described, and in Sec. III the modeling of the statistical γ cascades is discussed. The results of the measurements are then presented in Sec. IV and summarized in Sec. V.

II. EXPERIMENTAL SETUP AND MEASUREMENTS

A. Experimental setup

As already mentioned, the experiment was performed at the neutron source LANSCE [11]. The 800-MeV H^- beam from the LANSCE linac is injected into the proton storage ring where it is immediately converted to H^+ by stripping through a thin foil. The proton bunches are stacked for the entire linac macropulse. This pulsed beam is then extracted with a repetition rate of 20 Hz and strikes a tungsten spallation target. The resulting fast neutrons are moderated and sent to flight path 14 at the Manuel Lujan Jr. Neutron Scattering Center. The DANCE detector array is installed at 20 m on this flight path.

The DANCE spectrometer [12,13] is designed for studying neutron capture cross sections on small samples. It consists of 160 BaF_2 scintillation crystals surrounding a sample and subtending a solid angle of $\simeq 4\pi$. A ^{6}LiH shell about 6 cm thick is placed between the sample and the BaF_2 crystals to reduce the scattered neutron flux striking the crystals. The remaining background from scattered neutrons interacting with the BaF_2 crystals is subtracted in the off-line analysis.

Besides the BaF_2 crystals, the DANCE setup includes four additional detectors that are used to monitor the neutron flux. The target was a metal foil with a thickness of 25 mg/cm^2 enriched to 96.47% in ^{95}Mo.

B. Experimental spectra

Typical sum energy spectra from isolated resonances are shown in Fig. 1. Each spectrum consists of (i) a peak (the E_{total} peak) corresponding to the total energy available for the reaction

$$E_{\text{total}} = B_n + E_n, \tag{1}$$

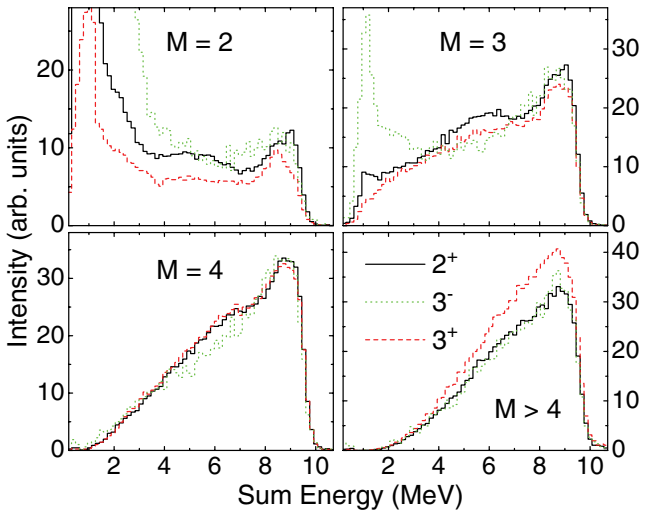

FIG. 1. (Color online) Examples of sum-energy spectra for resonances at energies of 160, 554, and 1361 eV with J^π assignments 3^+, 2^+, and 3^-, respectively. The multiplicities of the γ cascades, M, are indicated. The spectra are normalized to the intensity in the E_{total} peak for multiplicities $M = 2$–7.

where B_n is the neutron separation energy (which in our case is 9.154 MeV) and E_n is the energy of the incoming neutron in the center of mass, and (ii) a low-energy tail that corresponds to cascades for which a part of the emitted energy escaped the detector array. The shape of the spectrum at low sum energies (below about 3 MeV) is strongly influenced by the background, especially for low multiplicities.

For the analysis performed in this paper we have considered only events in the region of the E_{total} peak, namely for the detected sum energy $E_\Sigma = 7.6$–9.2 MeV. Detailed analysis was restricted to events that correspond to capture on well-isolated resonances with known spin and parity (see Ref. [10]).

C. Data processing

1. On-line data processing

The DANCE acquisition system [14] is based on waveform digitization of signals from all 160 detectors using four-channel Acqiris DC265 digitizers. Information is provided on timing, particle type, and energy for each event in the crystals. To handle both high and low amplitudes of the fast and slow components of the signals from the BaF_2 crystals separately, the signal from each of the detectors is processed by two digitizer channels with suitably adjusted gains. The digitizers are arranged in 14 compact PCI crates with six DC265 modules. Thus one crate can handle 12 BaF_2 detectors with two channels per detector. Each crate contains an embedded computer running under the Linux operating system and a front-end acquisition program written using the framework known as the Maximum Integrated Data Acquisition System (MIDAS) [15].

An external digitizer trigger signal is provided whenever the energy deposited in two or more crystals firing within a 100-ns time window exceeds a preset energy threshold. The intensity of both the fast and slow components of the signal from a specific crystal is collected. The ratio of these two components

is used for discrimination against the α background from radioactivity of natural impurities in the BaF_2 crystals [13].

2. Off-line data processing

Often the emitted capture γ rays do not deposit their full energy in one crystal. Therefore all contiguous crystals that have fired during an event are combined into one single "cluster" event. The cluster multiplicity is much closer to the true multiplicity of the γ cascade than is the "crystal" multiplicity (the total number of crystals that fire). The capture events in the off-line analysis were sorted by gates on each neutron resonance and on the cluster multiplicity.

The average multiplicity $\langle M \rangle$, the basic quantity characterizing the multiplicity distribution, was calculated as

$$\langle M \rangle = \frac{\sum_{M=2}^{7} M C_M}{\sum_{M=2}^{7} C_M}, \tag{2}$$

where C_M is the number of counts corresponding to multiplicity M after subtracting background contributions. The γ background in spectra for strong resonances is negligible for multiplicities $M > 1$. This is not true for the $M = 1$ spectra, where a background originating from γ rays following the capture of scattered neutrons in barium nuclei sometimes plays an important role. For this reason the multiplicity one counts, C_1, were omitted when calculating $\langle M \rangle$.

III. SIMULATIONS OF THE γ DECAY OF ^{96}Mo

A. Status

In the initial phase of our analysis the spins and parities of resonances in ^{96}Mo were determined [10]. This determination was based on analysis of the average multiplicity and the multiplicity distribution and on the shapes of what we call the multi-step cascade (MSC) γ-ray spectra. The difference in shapes of MSC spectra was very useful, especially for resolving 2^+ resonances from 3^- resonances and 3^+ resonances from 4^- resonances. For these cases the average multiplicity values are very close. Example MSC spectra for a typical 2^+ resonance and a typical 3^- resonance are shown in Fig. 2.

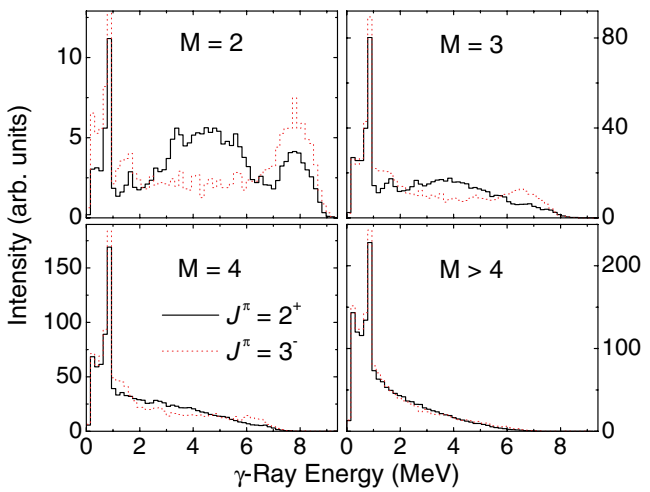

FIG. 2. (Color online) Experimental MSC spectra from a 2^+ resonances at 554 eV and a 3^- resonance at 1341 eV.

Once the parity of the resonances is established, the average multiplicities for the positive-parity states separate very clearly into two groups. These average multiplicities and the spread of these values for different resonances agree extremely well with statistical model calculations [10]. This provides additional confidence in the model calculations described in the following.

B. Simulations of spectra

To obtain information about the PSFs in ^{96}Mo, experimental γ-ray energy spectra were compared with results from simulations. The γ decay under different assumptions about the level density and PSFs was simulated by using the DICEBOX algorithm [16]. The response of the DANCE detector to the generated cascades was subsequently obtained with the help of a code based on the GEANT3 package. All material in the detector was included in the GEANT3 simulations. To verify the correctness of the GEANT3 simulations, tests were also performed with a code based on the GEANT4 package. It was found that results of both codes for simulation of the detector response were nearly identical.

The DICEBOX algorithm generates a complete decay scheme of an artificial nucleus. Below some critical energy, $E_{\rm crit}$, all the characteristics of the decay scheme (i.e., energies, spins, and parities of levels, as well as their decay properties) are taken from existing experimental data. The choice of the critical energy should be made with care to guarantee that all of the information for energies below $E_{\rm crit}$ is complete. We took the required data from Ref. [17] and adopted $E_{\rm crit} = 2.79$ MeV. Above $E_{\rm crit}$ the level system of the nucleus and its complete decay scheme are generated by using an *a priori* chosen level density function $\rho(E, J, \pi)$ and PSFs for multipolarities $E1$, $M1$, and $E2$. All higher multipolarities are neglected. Partial radiation widths for a transition between an initial level a and a final level b, $\Gamma_{a\gamma b}$, are given by

$$\Gamma_{a\gamma b} = \sum_{XL} \frac{\xi^2 f^{(XL)} E_\gamma^{2L+1}}{\rho(E_a, J_a, \pi_a)}, \tag{3}$$

where $f^{(XL)}$ stands for photon strength function for transitions of type X (electric or magnetic) and multipolarity L and ξ is a random number generated from a normal distribution with zero mean and unit variance. This random number ensures that the individual $\Gamma_{a\gamma b}$ fluctuate according to the Porter-Thomas distribution [18]. The sum in Eq. (3) is over all allowed types of transitions.

Hereafter the system of all levels and their decay scheme is called a *nuclear realization*. Owing to the Porter-Thomas fluctuations there is an infinite number of nuclear realizations that differ from each other even for fixed models of PSFs and level density.

Various models of PSFs and level density can be tested with the DICEBOX code. The fluctuations involved in generating the γ decay allow us to determine all of the inherent uncertainties that arise when simulations with the same models are performed. Cascades starting from resonances with a given spin and parity were simulated. Typically 20 nuclear realizations, each with 100,000 cascades, were simulated with the DICEBOX algorithm for initial resonance spins and

parities $J^\pi = 2^+, 3^+, 1^-, 2^-, 3^-, 4^-$. Spectra obtained from each nuclear realization were treated separately and were convoluted with a simulation of the detector response by using the GEANT3 package.

Various kinds of information can be obtained from the combined DICEBOX+GEANT simulations. Of special interest are the average multiplicities, the multiplicity distribution, and the γ-ray energy spectra for various multiplicities. Only one normalization coefficient is needed for comparison of γ-ray spectra for all multiplicities with experimental data. We normalized spectra to the same number of counts in the E_{total} peak, which includes almost all multiplicities (but in practice we consider $M = 2$–7).

C. Photon strength functions

It should be emphasized that using the DICEBOX algorithm we can easily test the acceptability of different models of PSFs and level density, but it is not possible to determine a "best" fit. Our procedure is essentially a trial-and-error approach. It should be emphasized that all the PSF models subject to our testing are implicitly assumed to comply with Brink's hypothesis [19].

1. Conventional model

The most straightforward approach is to adopt rather conventional phenomenological models that have been used for other nuclei. A model that reasonably well describes the experimental TSC spectra of ^{96}Mo [2] is given by

$$f(E_\gamma, T) = f_{E1}^{(\text{GLO})} + f_{M1}^{(\text{SF})} + f_{M1}^{(\text{SP})} + f_{E2}^{(\text{SP})}. \tag{4}$$

The single particle (SP) model, with $f^{(\text{SP})} = \text{constant}$, was assumed for the $E2$ PSF and for a part of the $M1$ PSF. The absolute values $f_{M1}^{(\text{SP})} = 1 \times 10^{-9}$ MeV^{-3} and $f_{E2}^{(\text{SP})} = 1.2 \times 10^{-12}$ MeV^{-5} were adopted in Ref. [2]. An additional resonance-like term, usually called the spin-flip (SF) term, with a Lorentzian shape,

$$f_{M1}^{(\text{SF})}(E_\gamma) = \frac{1}{3(\pi\hbar c)^2} \cdot \frac{\sigma_{\text{SF}}\, E_\gamma\, \Gamma_{\text{SF}}^2}{\left(E_\gamma^2 - E_{\text{SF}}^2\right)^2 + E_\gamma^2\, \Gamma_{\text{SF}}^2}, \tag{5}$$

was added to the $M1$ strength. The values 8.95 MeV, 4.0 MeV, and 1.5 mb were used for parameters E_{SF} (energy), Γ_{SF} (width), and σ_{SF} (maximum cross section of the resonance), respectively [20].

The semi-empirical GLO model [21], which was developed for description of spherical or weakly deformed nuclei, was used for the $E1$ PSF:

$$f_{E1}^{(\text{GLO})}(E_\gamma, T) = \frac{\sigma_G\, \Gamma_G}{3(\pi\hbar c)^2} \left[\frac{E_\gamma\, \Gamma(E_\gamma, T)}{\left(E_\gamma^2 - E_G^2\right)^2 + E_\gamma^2\, \Gamma(E_\gamma, T)^2} + \frac{4\pi^2\, F_K\, \Gamma_G\, T^2}{E_G^5} \right]. \tag{6}$$

Here E_G, Γ_G, and σ_G are the parameters of the giant dipole electric resonance, the factor $F_K = 0.7$ [20,22], and the temperature-dependent width $\Gamma(E_\gamma, T)$ is given by

$$\Gamma(E_\gamma, T) = \Gamma_G \frac{E_\gamma^2 + 4\pi^2 T^2}{E_G^2}, \tag{7}$$

with temperature $T = T(E) \equiv \sqrt{(E - \Delta)/a}$; E is the excitation energy of a final level, Δ is the pairing energy, and a is the shell-model level density parameter. The values $\Delta = 2.55$ MeV and $a = 10.19$ MeV^{-1} were adopted from Ref. [23].

The model given by Eq. (4) will be referred to as model A in the following. The shape of this model for the PSFs is shown in Fig. 3 as a gray band. The lower and upper bounds of this range are given by substituting, respectively, $T = 0$ and $T = \sqrt{(B_n - E_\gamma - \Delta)/a}$ into the right-hand side of Eq. (6).

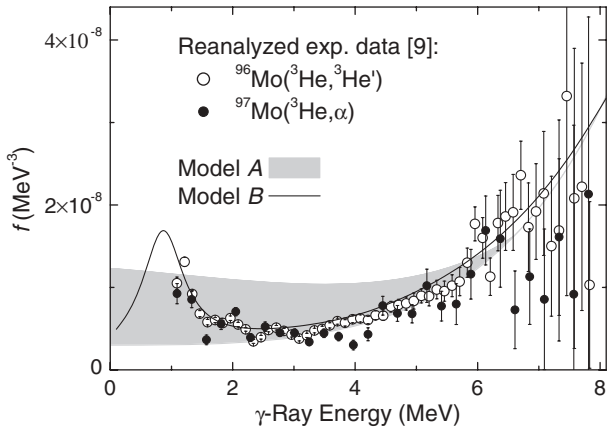

FIG. 3. Shapes of PSFs used in simulations.

2. The PSF deduced from ^{3}He-induced reactions

The PSF recommended in Ref. [6] has the form

$$f(E_\gamma, T) = \kappa\left[f_{E1}^{(\text{KMF})}(E_\gamma, T) + f_{M1}^{(\text{SF})}(E_\gamma) + f^{(\text{pole})}(E_\gamma)\right] + E_\gamma^2 f_{E2}^{(\text{GQER})}. \tag{8}$$

For the description of the $E1$ strength a model originally proposed by Kadmenskij, Markushev, and Furman (KMF) (see Ref. [22]) was adopted. The expression for the PSF following this model reads

$$f_{E1}^{(\text{KMF})}(E_\gamma, T) = \frac{F_K}{3(\pi\hbar c)^2} \cdot \frac{\sigma_G\, E_G \Gamma_G \Gamma(E_\gamma, T)}{\left(E_\gamma^2 - E_G^2\right)^2}. \tag{9}$$

The spin-flip (SF) model was adopted for the $M1$ PSF and the giant quadrupole electric resonance (GQER) term for the $E2$ PSF in Eq. (8). The shape of the GQER $E2$ term has the same form as the spin-flip $M1$ term [see Eq. (5)]. The only difference between $f_{\text{SF}}^{(M1)}$ and $f_{\text{GQER}}^{(E2)}$ is that the numerical factor 1/3 for dipole transitions is replaced by 1/5 for quadrupole transitions and a set of parameters $\{E_{\text{SF}}, \Gamma_{\text{SF}}, \sigma_{\text{SF}}\}$ by the set $\{E_{\text{GQER}} = 13.76$ MeV, $\Gamma_{\text{GQER}} = 4.96$ MeV, $\sigma_{\text{GQER}} = 2.21$ mb$\}$ [24].

In accordance with the parametrization introduced in Ref. [4] the enhancement term $f^{(\text{pole})}(E_\gamma)$ in Eq. (8) is given

by

$$f^{(\mathrm{pole})}(E_\gamma) = \frac{\mathcal{A}}{3(\pi\hbar c)^2} E_\gamma^{-b}. \quad (10)$$

Parameter κ in Eq. (8) is free, as well as $\mathcal{A}$ and b in Eq. (10). It should be emphasized again that, to provide a convenient way to characterize the data, the expression for $f^{(\mathrm{pole})}(E_\gamma)$ is purely empirical. Nevertheless, we did test the initial Oslo parametrization; this led to striking disagreement with the present DANCE data. This is consistent with the earlier TSC results [2].

The Oslo group has reanalyzed the ^{96}Mo data; the revised PSF data (Fig. 3) show significantly less enhancement at low γ-ray energies [9]. It was also suggested that the soft pole term $f^{(\mathrm{pole})}(E_\gamma)$ be replaced by a resonance term at low excitation energies, $f_R(E_\gamma)$. Specifically, the Lorentzian represented by Eq. (5) was adopted for $f_R(E_\gamma)$, with the set of parameters $\{E_{\mathrm{SF}}, \Gamma_{\mathrm{SF}}, \sigma_{\mathrm{SF}}\}$ replaced by the set $\{E_R = 0.95$ MeV, $\Gamma_R = 0.77$ MeV, $\sigma_R = 0.14$ mb$\}$ [9]. This model will be referred to as model B and the corresponding PSF is also plotted in Fig. 3.

D. Nuclear level density

We used almost exclusively the back-shifted Fermi gas (BSFG) model [23]

$$\rho(E, J, \pi) = f(J) f(\pi) \frac{e^{2\sqrt{a(E-E_1)}}}{12 \cdot 2^{1/2}\, \sigma_c\, a^{1/4} (E - E_1)^{5/4}}, \quad (11)$$

where a and E_1 are adjustable parameters and

$$f(J) = \exp\left(\frac{-J^2}{2\sigma_c^2}\right) - \exp\left(\frac{-(J+1)^2}{2\sigma_c^2}\right) \quad (12)$$

is the spin probability distribution function. For the spin cutoff parameter σ_c we used the expression given in Ref. [23]:

$$\sigma_c^2 = 0.0888 A^{2/3} \sqrt{a(E - E_1)}. \quad (13)$$

This parametrization is consistent with that used in the analysis by the Oslo group [6] and in the description of the TSC data [2]. The values of parameters a and E_1 were set to 10.19 MeV^{-1} and 0.71 MeV [23], respectively. We also repeated the calculations with a different spin cutoff value that was adopted in a recent level density compilation [25]. In this case, the values of parameters a and E_1 were set to 10.90 MeV^{-1} and 0.59 MeV, respectively. Calculations with this slightly adjusted level density expression will be called model $A^\dagger$ in the following.

The level density at high excitation energies is expected to be parity independent, which corresponds to $f(\pi) = 0.5$ in Eq. (11). However, the parity dependence at low energies remains in question. Level schemes from other experiments [17] show significant parity asymmetry below about 3 MeV. Therefore, instead of using a parity-independent level density above E_{crit}, we normally used the formula from Ref. [26],

$$f(\pi = +) = \frac{1}{2}\left(1 + \frac{1}{1 + \exp\left[C_\pi (E - \Delta_\pi)\right]}\right), \quad (14)$$

where Δ_π is, roughly speaking, the excitation energy at which the parity-dependent level density changes to being parity independent, with the rate given by C_π. For the negative-parity level density the relation $f(\pi = -) = 1 - f(\pi = +)$ was used. The parameters characterizing the parity dependence of the level density were set to $\Delta_\pi = 3.2$ MeV and $C_\pi = 1.0$ MeV^{-1} [26]. To check the possible influence of the parity dependence of level density on the γ decay, we also performed simulations with $f(\pi) = 1/2$ for all energies above E_{crit}. The spin cutoff parameter from Ref. [23] was used in this simulation, which will be labeled model A^* in the following.

We note that the level density obtained from the Oslo measurements [7] is in excellent agreement with the adopted level density model.

IV. RESULTS AND DISCUSSION

The experimental MSC spectra for different resonances with the same spin and parity are essentially the same; this is illustrated in Fig. 4, where spectra for various multiplicities are shown for several strong $J^\pi = 2^+, 2^-, 3^+$, and 3^- resonances. For clarity, in the following comparisons between model calculations and the experimental spectra shown we include only one typical resonance of the appropriate spin and parity. As noted earlier, the events included in the MSC spectra are those for which the detected sum energy is in the energy range 7.6–9.2 MeV.

First we compared simulations with model A. The results are shown in Fig. 5. To minimize statistical uncertainties as well as uncertainties from simulations, the spectra were binned into coarse bins with a width of 150 keV. Simulated MSC spectra from different nuclear realizations obtained with the same model of PSFs and level density are not identical, but instead fluctuate. This is a consequence of fluctuations involved in generating the partial radiative widths. To characterize these fluctuations the simulation predictions are plotted as a gray band. This band has a width of two sigma (the average $\pm$ one sigma) and was obtained from analysis of 20 independent nuclear realizations.

It should be noted that there are two different kinds of uncertainties in the simulations of spectra from different resonances with the same J^π. First, different partial radiative widths of primary transitions from different resonances to the same low-lying levels lead to slightly different spectral shapes of spectra and average multiplicities from these resonances. This type of uncertainty is not only connected with simulations, but it is also inherent in experimental spectra, as shown in Fig. 4. An additional uncertainty is associated with uncertainties about the decay patterns of secondary transitions. This is related only to simulations, where different nuclear realizations simulate this uncertainty. Both of these uncertainties can be correctly simulated with the DICEBOX code. Uncertainties of the second kind, which inherently include those of the first kind, are shown in the figures. It turns out that uncertainties of the first type dominate.

MSC spectra originating from decay of resonances with six different spin-parity combinations in the ^{96}Mo compound nucleus were obtained. Spectra from 2^+, 3^+, 1^-, 2^-, 3^-, and 4^- resonances were compared. As Fig. 5 shows, the DICEBOX

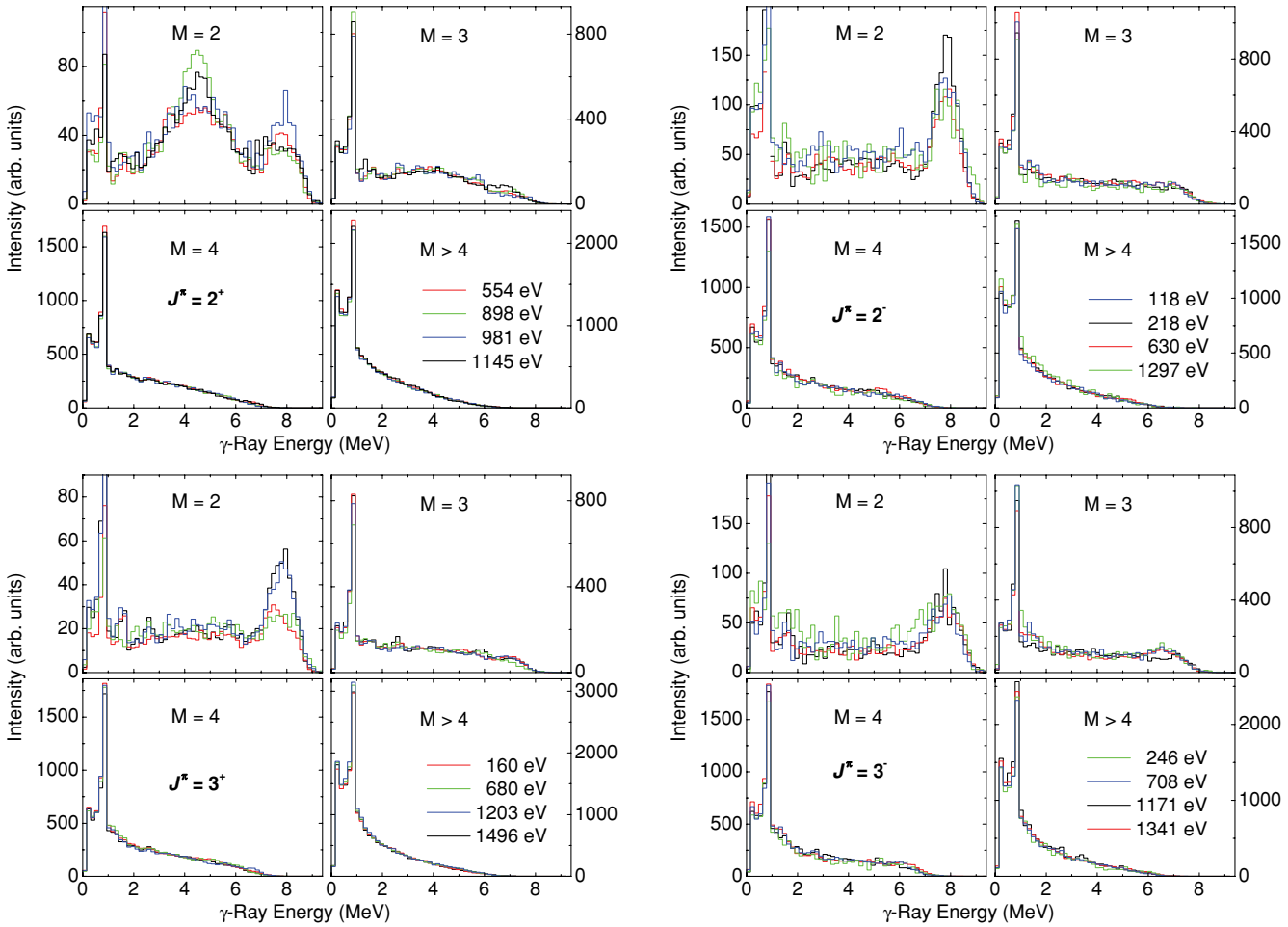

FIG. 4. (Color online) Experimental MSC spectra from different resonances. Energies of resonances are indicated.

simulations using model A agree well with the experimental spectra for resonances with different J^π assignments, in particular for p-wave resonances with $J = 2$–4. In this context we emphasize that the model parameters have not been adjusted to describe the present data. Instead, all parameters used were deduced from fitting the TSC ^{96}Mo data on the γ decay of the $J^\pi = 3^+$ thermal neutron capturing state of the system $^{95}\mathrm{Mo} + n$ [2]. We would like to stress again that there is only one common normalization factor for all multipolarities used for comparison of simulations with experimental data.

One feature of our data is disturbing: an unexpected underestimate of the intensities at energies $E_\gamma < 1$ MeV (and, as a consequence of the inherent symmetry, also at $E_\gamma > B_n - 1$ MeV) in the multiplicity two MSC spectrum for the only available strong p-wave resonance with $J^\pi = 1^-$ at 110.4 eV (see Fig. 5). One can speculate that the observed extra strength originates from the direct neutron capture of the type $p \rightarrow s$ or $p \rightarrow d$. However, although the reduced neutron widths of some of the p-wave resonances with $J > 1$ included in our analysis are higher by a factor of 2–8 compared to the reduced neutron width of the $J^\pi = 1^-$ resonance at 110.4 eV, no extra strength at the beginning and end of multiplicity two spectra is observed for these resonances. Thus, it does not seem that the direct capture accounts for the observed anomaly at the 110.4-eV resonance.

As noted in Sec. III, the Oslo group recently reanalyzed the data on ^{96}Mo and obtained a revised PSF (model B—see Fig. 3) with a reduced low-energy enhancement [9]. A comparison of DICEBOX simulations using this revised PSF with the DANCE experimental results is shown in Fig. 6. The agreement with the experimental data is comparable to that obtained with our conventional model A.

The experimental data for the γ decay in ^{96}Mo are consistent with a conventional set of PSFs and level density that fit the TSC data of Ref. [2]. These data are not consistent with the large enhancement of the PSF proposed by the Oslo group. However, our experimental data are not sufficiently sensitive to distinguish between a *small* low-energy enhancement (Oslo model B) and *no* enhancement (Řež model A).

The shapes of MSC spectra for models $A^\dagger$ and A^* are very similar to the spectra obtained with model A. This suggests that our results are insensitive to details of the level density model.

These conclusions are based on visual examination of the MSC spectra. Some basic features of the multiplicity distributions can be characterized by the average multiplicity $\langle M_J \rangle$. The results of the model calculations for the average multiplicity are shown in Table I.

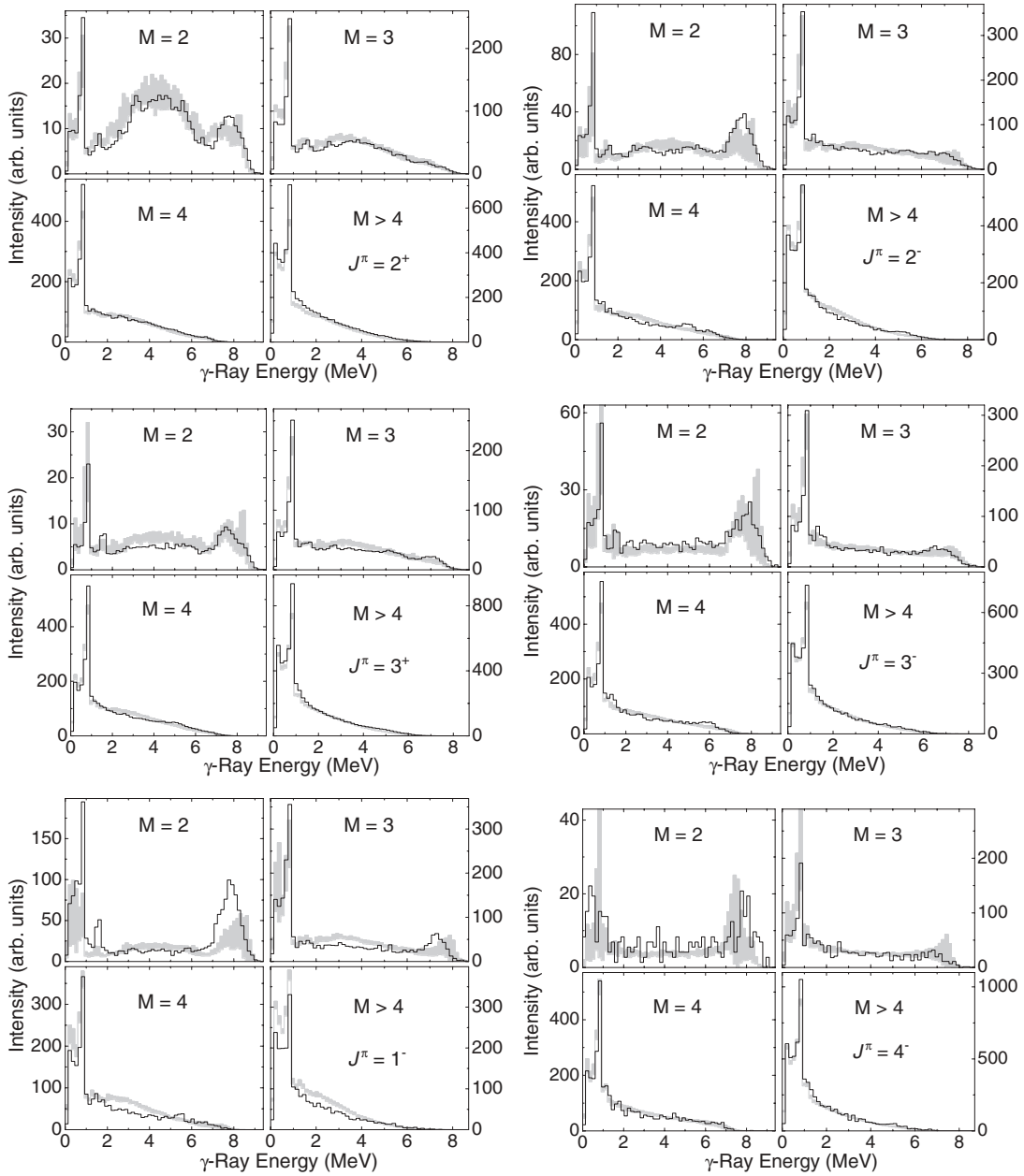

FIG. 5. Comparison of simulated MSC spectra using model A (gray regions) with the experimental data for selected resonances (histograms). Resonances with energies of 554, 160, 110, 630, 708, and 1788 eV were used for comparison with simulation for 2^+, 3^+, 1^-, 2^-, 3^-, and 4^-, respectively. The PSF that was used in simulations is shown in Fig. 3 as a gray band.

TABLE I. Average multiplicities of spectra from resonances with various initial spins and parities.

Model	Average multiplicity $\langle M_J \rangle$					
	2^+	3^+	1^-	2^-	3^-	4^-
A	3.87(3)	4.15(3)	3.57(10)	3.78(8)	3.96(6)	4.26(11)
A^*	3.86(2)	4.11(4)	3.54(14)	3.74(16)	3.96(11)	4.25(14)
$A^\dagger$	3.87(5)	4.19(3)	3.57(10)	3.81(8)	4.04(8)	4.35(4)
B	4.02(4)	4.25(4)	3.80(10)	3.99(8)	4.14(6)	4.40(11)
Exp.	3.95(3)	4.27(4)	3.41(7)	3.74(7)	4.03(6)	4.40(7)

The average multiplicities for negative-parity resonances have significantly larger uncertainties that arise from Porter-Thomas fluctuations. This is true for both the experimental data and for the simulations. The overall agreement between the predicted average multiplicity values and the predictions from our model A (and its modifications $A^\dagger$ and A^*) is reasonable, but still not ideal. The predictions for model B agree reasonably well with experiment, consistent with the conclusions from visual inspection of the energy spectra. The various models adjusting the level density parameters seem to yield very similar results.

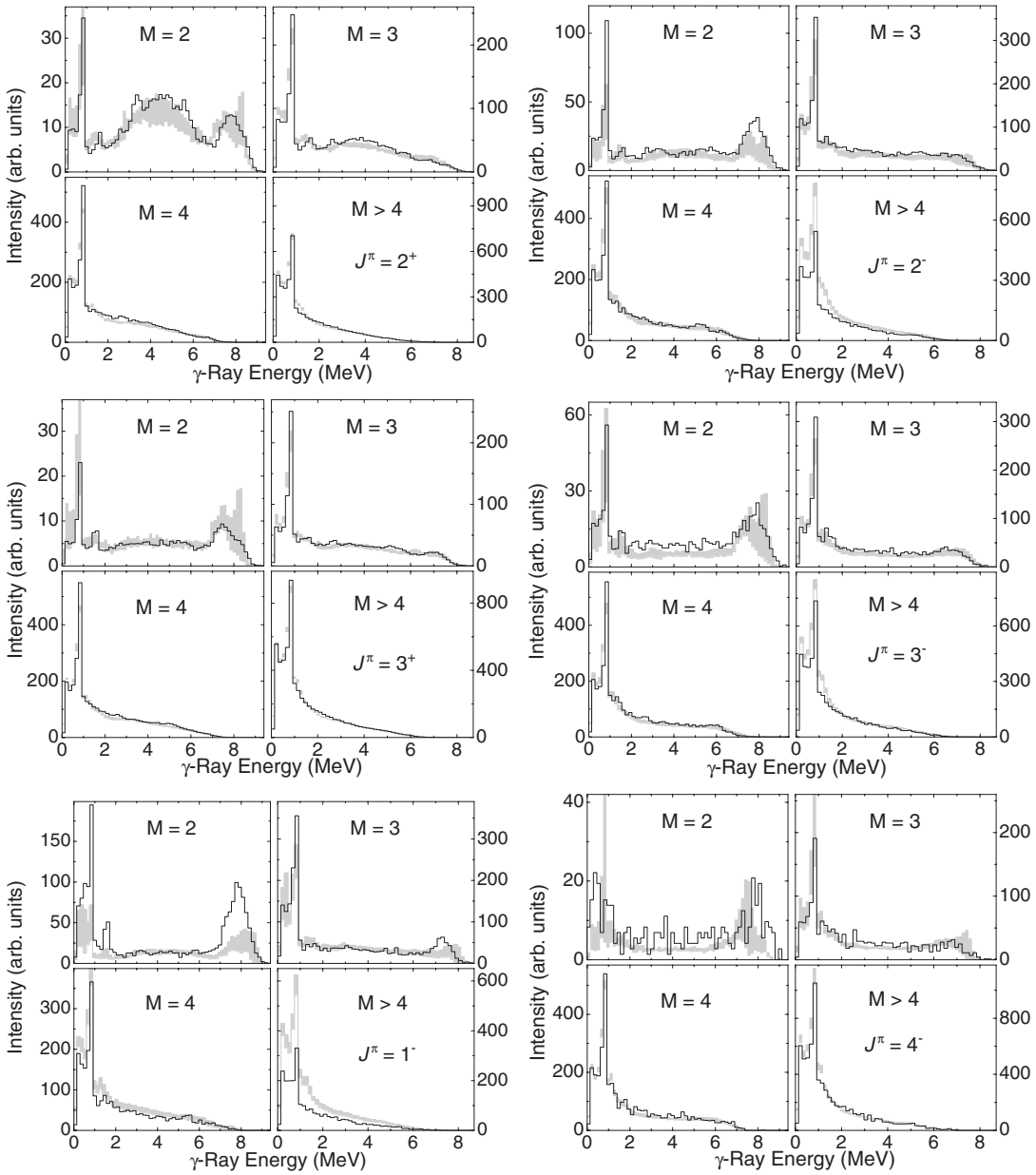

FIG. 6. Comparison of simulated MSC spectra using model *B*—the new Oslo model—with the experimental capture data. The experimental data are taken from the same resonances as those indicated in Fig. 5. The PSF that was used in the simulations is shown in Fig. 3 as a solid curve.

Another quantity that can be easily obtained from simulations is the total radiative width Γ_γ. Values of this quantity for all available resonance spin-parity combinations are listed for models A, $A^\dagger$, and A^* in Table II. Simulations are not included for model B based on the Oslo results, because their method requires normalizing the PSFs to reproduce the experimental value of Γ_γ. Again our conventional model A provides reasonable agreement with the experimental values.

Based on the evidence from extensive comparison with model simulations, it seems safe to conclude that the DANCE and Řež data are not consistent with a large enhancement at low energies for the photon strength function according to the approximation given by Eq. (10). Both data sets are consistent with no enhancement. However, the existence of a much weaker enhancement at low energies cannot be ruled out from the present DANCE experimental results.

TABLE II. Simulated total radiative width of resonances for different models. Experimental values of Γ_γ for s- and p-wave resonances are equal to 162(7) and 210(40) meV, respectively [27].

Model	Total radiative width (meV)					
	2^+	3^+	1^-	2^-	3^-	4^-
A	151(4)	143(5)	223(35)	193(13)	186(8)	168(9)
A^*	165(5)	160(4)	214(38)	187(19)	179(18)	162(12)
$A^\dagger$	137(6)	128(7)	187(23)	163(11)	164(13)	150(6)

V. SUMMARY

Measurements of the multi-step γ cascades following neutron resonance capture in an isotopically enriched ^{95}Mo sample were performed with the DANCE detector array at LANSCE by the time-of-flight method.

The MSC γ-ray spectra for different multiplicities from resonances with different spin and parity were used for testing the validity of various PSF models. Our simulations indicate that decay of compound nuclei in the molybdenum region can be described by the extreme statistical model. This conclusion is in good agreement with the results of the TSC measurements in the ^{96}Mo compound nucleus following thermal neutron capture [2]. Models of PSFs that reproduce TSC spectra well are also able to describe spectra from isolated resonances well. These models contain no enhancement of PSFs at low energies, although the present data do not rule out a weak enhancement of PSFs. The extreme statistical model appears to work very well in the compound nucleus ^{96}Mo.

To clarify the role of possible nonstatistical effects in MSCs involving very low lying levels, as suggested by the MSC spectrum for the $J^\pi = 1^-$ p-wave resonance at 110.4 keV, additional data from high-resolution measurements of spectra of primary γ rays at isolated neutron resonances of ^{95}Mo are needed.

The theory of Kadmenskij, Markushev, and Furman [22] represents the main ingredient of the model *A* that successfully describes our data. To our knowledge the ^{96}Mo nucleus represents the best example for which this theory works well. However, the KMF theory is by no means generally accepted. Existing literature (e.g., Refs. [28,29]) suggests that the $E1$ PSF of deformed nuclei can be reasonably described by a simple Brink-Axel model [19,30] according to which the cross section for photoabsorption by an *excited* target is given by a superposition of Lorentzians with energy- and temperature-independent damping widths Γ_G. This leads us to make a concluding remark: After more than a half century we still do not have a fully quantitative or universally applicable theory of γ decay of slow-neutron capturing states.

ACKNOWLEDGMENTS

This work was supported in part by the US Department of Energy Grant Nos. DE-FG52-06NA26194 and DE-FG02-97-ER41042 and was performed under the auspices of the US Department of Energy by the University of California, Lawrence Livermore National Laboratory and Los Alamos National Laboratory under Contract Nos. W-7405-ENG-48 and W-7405-ENG-36, respectively. This work has benefited from the use of the LANSCE accelerator facility, supported under DOE Contract No. DE-AC52-06NA25396. It was also supported by the research plans MSM 0021620859 and INGO LA08015 of the Ministry of Education of the Czech Republic.

[1] R. E. Chrien, G. W. Cole, G. G. Slaughter, and J. A. Harvey, Phys. Rev. C **13**, 578 (1976).
[2] M. Krtička, F. Bečvář, I. Tomandl, G. Rusev, U. Agvaanluvsan, and G. E. Mitchell, Phys. Rev. C **77**, 054319 (2008).
[3] E. Tavukcu, Ph.D. thesis, North Carolina State University (2002).
[4] A. Voinov *et al.*, Phys. Rev. Lett. **93**, 142504 (2004).
[5] A. C. Larsen *et al.*, Phys. Rev. C **73**, 064301 (2006).
[6] M. Guttormsen *et al.*, Phys. Rev. C **71**, 044307 (2005).
[7] R. Chankova *et al.*, Phys. Rev. C **73**, 034311 (2006).
[8] A. C. Larsen *et al.*, Phys. Rev. C **76**, 044303 (2007).
[9] M. Guttormsen (private communication).
[10] S. A. Sheets *et al.*, Phys. Rev. C **76**, 064317 (2007).
[11] P. W. Lisowski *et al.*, Nucl. Sci. Eng. **106**, 208 (1990).
[12] M. Heil, R. Reifarth, M. M. Fowler, R. C. Haight, F. Käppeler, R. S. Rundberg, E. H. Seabury, J. L. Ullmann, and K. Wisshak, Nucl. Instrum. Methods Phys. Res. A **459**, 229 (2001).
[13] R. Reifarth *et al.*, Nucl. Instrum. Methods Phys. Res. A **459**, 229 (2001).
[14] J. M. Wouters *et al.*, IEEE Trans. Nucl. Sci. **53**, 880 (2006).
[15] S. Ritt and P.-A. Amaudruz, MIDAS—Maximum Integrated Data Acquisition System, http://midas.psi.ch.
[16] F. Bečvář, Nucl. Instrum. Methods Phys. Res. A **417**, 434 (1998).
[17] L. K. Peker *et al.* Nucl. Data Sheets **68**, 165 (1993).
[18] C. E. Porter and R. G. Thomas, Phys. Rev. **104**, 483 (1956).
[19] D. M. Brink, Ph.D. thesis, Oxford University (1955).
[20] J. Kopecky, in *Handbook for Calculations of Nuclear Reaction Data*, Report No. IAEA-TECDOC-1034 (IAEA, Vienna, 1998), p. 97.
[21] J. Kopecky and M. Uhl, Phys. Rev. C **41**, 1941 (1990), and references therein.
[22] S. G. Kadmenskij, V. P. Markushev, and V. I. Furman, Sov. J. Nucl. Phys. **37**, 165 (1983).
[23] T. von Egidy, H. H. Schmidt, and A. N. Behkami, Nucl. Phys. **A481**, 189 (1988).
[24] W. V. Prestwich, M. A. Islam, and T. J. Kennett, Z. Phys. A **315**, 103 (1984).
[25] T. von Egidy and D. Bucurescu, Phys. Rev. C **72**, 044311 (2005).
[26] S. I. Al-Quraishi, S. M. Grimes, T. N. Massey, and D. A. Resler, Phys. Rev. C **67**, 015803 (2003).
[27] S. F. Mughabghab, *Atlas of Neutron Resonances* (Elsevier, Amsterdam, 2006).
[28] S. Raman, in *Neutron Capture Gamma-Ray Spectroscopy and Related Topics: Proceedings of the Fourth International Symposium on Neutron-Capture Gamma-Ray Spectroscopy*, edited by F. Gönenwein, T. von Egidy, and G. Maier (Institute of Physics, London, 1982), Vol. 62, p. 357.
[29] S. Kahane, S. Raman, G. G. Slaughter, C. Coceva, and M. Stefanon, Phys. Rev. C **30**, 807 (1984).
[30] P. Axel, Phys. Rev. **126**, 671 (1962).